TÜBİTAK

Turkish Journal of Medical Sciences

http://journals.tubitak.gov.tr/medical/

Research Article

Turk J Med Sci
(2015) 45: 18-26
© TÜBİTAK
doi:10.3906/sag-1308-48

PARP inhibition prevents acetaminophen-induced liver injury and increases survival rate in rats

Melahat DÖNMEZ[1,*], Bülent UYSAL[2], Yavuz POYRAZOĞLU[3], Yeşim ER ÖZTAŞ[4], Türker TÜRKER[5], Ümit KALDIRIM[6], Ahmet KORKMAZ[2]

[1]Department of Pathology, Ministry of Health, Dışkapı Yıldırım Beyazıt Training and Research Hospital, Ankara, Turkey
[2]Department of Physiology, Gülhane Military Medical Academy, Etlik, Ankara, Turkey
[3]Department of General Surgery, Mevki Military Hospital, Ankara, Turkey
[4]Department of Medical Biochemistry, Faculty of Medicine, Hacettepe University, Sıhhiye, Ankara, Turkey
[5]Department of Public Health, Gülhane Military Medical Academy, Etlik, Ankara, Turkey
[6]Department of Emergency Medicine, Gülhane Military Medical Academy, Etlik, Ankara, Turkey

Received: 15.08.2013 • **Accepted:** 08.10.2013 • **Published Online:** 12.01.2015 • **Printed:** 09.02.2015

Background/aim: Acetaminophen (APAP) overdose results in severe liver damage that may develop into acute liver failure. Recent studies have demonstrated that inhibition of poly(ADP-ribose) polymerase (PARP) decreases tissue necrosis and inflammation. We evaluated the efficacy of 3-aminobenzamide (3-AB), a PARP inhibitor, in a rodent model of APAP-induced hepatotoxicity.

Materials and methods: Twenty-four Sprague-Dawley rats were divided equally into 3 experimental groups: sham group, APAP group, and APAP + 3-AB group. In the experimental treatment groups APAP was administered orally at 1 g/kg and, in the APAP + 3-AB group, 3-AB was administered intraperitoneally at a dose of 20 mg/kg exactly 1 h after APAP treatment. Surviving animals were euthanized 48 h after initial APAP administration. Blood samples and liver tissues were collected for histopathological and biochemical analysis.

Results: A panel of oxidative stress parameters, as well as serum aspartate aminotransferase, alanine aminotransferase, neopterin, and nitrite/nitrate and histological injury scores, were significantly reduced among the APAP + 3-AB treatment group relative to the group treated with APAP alone ($P < 0.05$, APAP vs. APAP + 3-AB).

Conclusion: The present study demonstrates that 3-AB inhibited APAP-induced hepatic injury and reduced neopterin levels. Results of the present study indicate that PARP inhibitors may be an effective adjuvant therapy resulting in improved outcomes in APAP-induced hepatotoxicity.

Key words: Acetaminophen, toxicity, PARP inhibition, neopterin, nitrosative stress, oxidative stress

1. Introduction

Acetaminophen (N-acetyl-para-aminophenol, APAP) is a commonly used analgesic medication with potent antiinflammatory effects. Although it is considered safe at therapeutic doses, excessive doses of APAP may result in severe centrilobular liver injury with potentially fatal results, including fulminant hepatic failure (1,2).

APAP overdose is clinically significant as APAP is the most common cause of drug-induced liver failure in the United States and Great Britain (3). In addition, animal models of APAP overdose have been used extensively to evaluate novel hepatoprotective agents. The mechanism of APAP-induced hepatic damage has been well characterized in both animals and humans (4–6). Initial morphological changes to the liver following APAP overdose include glycogen loss and vacuolization of centrilobular hepatocytes, hepatocyte nuclear distortion, and single-cell necrosis with pyknotic nuclei exhibiting eosinophilic degeneration. In more advanced stages, the centrilobular zones of the liver exposed to severe toxic injury exhibit massive necrosis including confluent zones of anuclear, eosinophilic hepatocytes. This damage has been predominantly attributed to the active metabolite of APAP, N-acetyl-para-benzoquinoneimine (NAPQI), which depletes cytoplasmic glutathione (GSH) stores and forms nonspecific covalent bonds with macromolecules that lead to dysfunction and eventual cell death (5). In addition, APAP enhances generation of reactive oxygen intermediates that contribute significantly to hepatotoxicity (7,8).

* Correspondence: mdonmezm@gmail.com

At therapeutic dosages APAP is excreted efficiently in nontoxic glucuronic acid and sulfate conjugates (9). Only a small percentage of APAP is converted to NAPQI by cytochrome P-450–mediated oxidases when used at recommended dosages. In the reduced form, intracellular GSH is conjugated to NAPQI, the detoxifying main byproduct of APAP metabolism (10,11). APAP toxicity at high dosages involves metabolic activation and the formation of a reactive metabolite, presumably NAPQI (12). However, exhaustion of intracellular GSH enables covalent conjugation of NAPQI with cellular proteins (4,13), including mitochondrial macromolecules (14,15). Mitochondrial dysfunction occurs as a result of the inhibition of mitochondrial respiration by NAPQI conjugates (16,17), increasing mitochondrial oxidant stress and peroxynitrite formation (18–20). As a result, the amount of available ATP decreases (16,19) and mitochondrial cytochrome c is released (21,22). Mitochondrial permeability and the collapse of the mitochondrial membrane result in necrotic cell death (4,23).

DNA fragmentation and mitochondrial dysfunction are early events in the pathogenesis of APAP toxicity (24,25). Shen et al. demonstrated that DNA fragmentation is a significant process in the cell injury and that the application of a general endonuclease inhibitor prevents DNA fragmentation and protects against APAP-induced liver injury (26). The precise role of endonucleases has not yet been identified; however, current evidence suggests that endonucleases may play a more important role than caspase-activated desoxyribonuclease (CAD) in disease pathogenesis. APAP overdose has not been associated with CAD activation (21,27,28), and the DNA fragments generated during APAP-induced toxicity differ substantially from those generated during caspase-dependent apoptosis (29).

Poly(ADP-ribose) polymerase (PARP) catalyzes the modification of nuclear proteins by poly-ADP ribosylation. PARP is central to the cellular response to DNA damage and is activated by severe DNA injury. Extensive PARP activation exhausts the intracellular nicotinamide adenine dinucleotide (NAD) pool, an essential metabolic cofactor required in the mitochondrial electron transport chain (30). DNA repair processes are inhibited in the absence of sufficient energetic resources, resulting in cellular dysfunction and necrotic cell death. PARP plays a significant role as a mediator of cell death and subsequent tissue injury and cellular dysfunction. Oxidative/nitrosative stress is also a significant factor in the pathogenesis of liver toxicity (31). PARP contributes to the escalation of inflammatory processes and the pharmacological inhibition of PARP functions has been demonstrated to suppress the expression of inflammatory mediators including cytokines, chemokines, and cellular adhesion molecules (32). To date, numerous pharmacologic agents and various molecular mechanisms have been examined in the attempt to develop new therapeutic approaches to overdose-related APAP toxicity. Among these mechanisms of action is PARP activation. APAP overdose induces DNA fragmentation and the subsequent excessive activation of PARP (33). Interestingly, PARP antagonists have been demonstrated to protect against APAP hepatotoxicity in mice (34). PARP inhibitors have also been evaluated as potent antiinflammatory agents (35,36).

Pharmacologic inhibition of PARP has proven to be an effective treatment for a variety of disease processes, including cancer. Certain cancer cell lineages are highly dependent on PARP, much more so than comparable healthy cells, making PARP an attractive target for cancer therapy. PARP inhibitors have also been considered as a potential treatment for acute life-threatening diseases, including stroke and myocardial infarction, as well as long-term neurodegenerative disease (37).

3-Aminobenzamide (3-AB) is a well-known inhibitor of PARP (38). PARP activation depletes intracellular stores of NAD (39). 3-AB is a close NAD^+ analog capable of binding PARP at the active site and inhibiting NAD^+ depletion. 3-AB may have potential as an anticancer drug (39).

Delayed medical treatment for APAP overdose is associated with increased mortality and significant clinical complications. In an attempt to address the deficits in current medical therapy for APAP overdose, we evaluated the efficacy of the PARP inhibitor 3-AB on hepatotoxic injury and mortality due to APAP overdose in rats.

2. Materials and methods

2.1. Animals and study groups

The Institutional Committee on the Care and Use of Animals reviewed and approved all animal procedures conducted in this study (Issue 09/67, 09.11.2009). Twenty-four male Sprague-Dawley rats (200–250 g) bred in the animal laboratory of our institution were randomly divided into 3 equal groups: sham group (N = 8), APAP group (N = 8), and APAP treatment with 3-AB therapy group (N = 8). Prior to the experiment the animals were fed with standard rat chow diet and given water ad libitum, and the animals were housed in cages with controlled temperature and a 12-h light/dark cycle for at least 1 week.

2.2. Induction of hepatotoxicity

A suspension of APAP (Pharmaceutical Factory of Turkish Armed Forces, Ankara, Turkey) was prepared in warm distilled water and administered to experimental rats at a dose of 1 g/kg by oral gavage as previously described (40). Following APAP administration, the animals were returned to their cages to recover. Water and food were available ad libitum.

2.3. Treatment procedure

In the treatment procedure, 20 mg/kg 3-AB was administered intraperitoneally once daily for 2 days starting 1 h after the induction of toxicity with APAP in the rats in the APAP + 3-AB experimental group.

2.4. Sample collection

All the surviving animals were anesthetized for laparotomy at 48 h after hepatotoxic induction. Blood samples were obtained for biochemical analyses by cardiac punctuation, and serum was obtained by centrifugation of the whole blood samples. The liver tissues were harvested for histological and biochemical analysis. A section of liver tissue from each animal was fixed in 10% formalin for histopathological evaluation, and the remaining liver tissue samples were stored at –80 °C for future measurement of antioxidant enzyme activity and tissue lipid peroxidation. All experimental animals were euthanized by decapitation.

2.5. Tissue preparation and biochemical analysis

Liver tissue samples were homogenized in ice-cold phosphate buffered saline (pH 7.4) using a homogenizer (Heidolph Diax 900; Heidolph Elektro GmbH, Kelheim, Germany). The resulting supernatant was used for all biochemical assays. The protein content of the tissue homogenates was measured using the Lowry method with bovine serum albumin as the standard protein (41).

The overall level of lipid peroxidation was measured using the thiobarbituric acid (TBA) reaction (42). A spectrophotometric measurement at 535 nm was used to quantify the reaction products of TBA and malondialdehyde (MDA). The calculated MDA levels are expressed as nM/mg protein.

Superoxide dismutase (SOD) activity was assayed using the nitroblue tetrazolium (NBT) method as described previously (43). This method is based on the reduction of NBT to blue formazan by $\cdot O_2^-$, which has strong absorbance at 560 nm. One unit of SOD is defined as the amount of protein that inhibits the rate of NBT reduction by 50%. The estimated SOD activity is expressed as U/g protein.

Glutathione peroxidase (GSH-Px) activity was measured using a method described previously (44). Briefly, GSH-Px activity was coupled to the oxidation of nicotinamide adenine dinucleotide phosphate (NADPH) by glutathione reductase. The oxidation of NADPH was quantified by spectrophotometric measurement at 340 nm and 37 °C for 5 min. GSH-Px activity is calculated as the slope of the line or as mM NADPH oxidized per minute. GSH-Px activity is presented as U/g protein.

Serum aspartate aminotransferase (AST), alanine aminotransferase (ALT), alkaline phosphatase (ALP), and gamma-glutamyl transferase (GGT) concentrations were measured by a spectrophotometric technique using an Olympus AU-2700 autoanalyzer and commercially available kits (Olympus, Hamburg, Germany) and are expressed as U/L.

Serum neopterin (NP) concentrations were determined using high-pressure liquid chromatography (Agilent Technologies 1200 Series System, Santa Clara, CA, USA) with a fluorescence detector as described previously (45). In brief, 0.1 mL of 2 mmol/L trichloroacetic acid was added to 0.4 mL of serum or tissue supernatant and the mixture was cooled in an ice bath for 10 min. The precipitated protein was removed by centrifugation at 2000 × *g* for 10 min. Twenty microliters of the supernatant was filtered through a 0.2 mm filter and injected into the chromatographic system. Separation of NP was achieved with a 250 × 4.6 mm^2 ID Allsphere ODS-2, C18 RP column with a particle size of 5 mm (Alltech, Deerfield, IL, USA) fitted with a 10 × 4.6 mm^2 ID Allsphere ODS-2 guard column (Alltech) using 0.015 mM/L phosphate buffer (pH 6.4) as the mobile phase (isocratic elution) at a flow rate of 0.8 mL/min. The peaks detected by the fluorescent detector (Ex: 353 nm; Em: 438 nm) were used for quantification. Serum neopterin concentrations are expressed as nM/L.

2.6. Serum nitrite-nitrate (NOx)

Serum samples were passed through 0.45 μm pore membrane nitrocellulose filters prior to NOx analysis. NOx levels were detected by means of an ion chromatograph (Dionex ICS-1000, Sunnyvale, CA, USA). Anion and guard columns (AS-9HC/AG-9HC, CS12A/CG12A, Dionex) and automated suppression were used. NOx levels were quantified using separate standard solutions for each ion and are expressed as mg/L (46).

2.7. Histopathologic analysis

Tissue specimens were fixed in 10% formalin for 24 h, then embedded in paraffin and cut into sections 5 μm thick. Slides were stained with hematoxylin and eosin (H&E) and examined under a light microscope. Each slide was evaluated by an expert investigator blinded to the identity of the experimental groups and liver injury was scored according to the method previously described by Gul et al. (47). Liver injury was scored for the degree of edema (0–4), inflammatory infiltration (0–6), hemorrhage (0–6), and ballooning (prenecrotic degeneration; 0–8). The total area of edema, infiltration, hemorrhage, and ballooning was also taken into account. The summation of the individual histological parameters resulted in a single score per slide with a maximum score of 24.

2.8. Statistical analysis

Results are expressed as median (min–max). Normality of the sampling distribution was analyzed using the Kruskal–Wallis test. Comparison between groups was conducted using the Mann–Whitney U test. $P < 0.05$ was considered statistically significant. All analyses were performed using SPSS 11.0 (SPSS Inc., Chicago, IL, USA).

3. Results

3.1. Animals

Over the course of the experimental treatment, 3 of 8 rats in the APAP group died (1 and 2 animals at the 24th and 36th hours, respectively), while all animals in the sham treatment and APAP + 3-AB experimental groups survived until the end of the experiment (Figure 1). The overall survival in the APAP + 3-AB treatment group was significantly greater than that of the rats treated with APAP alone (P = 0.025).

3.2. Serum ALT and AST activities

Serum ALT and AST levels were significantly elevated in the APAP treatment group relative to the sham treatment and APAP + 3-AB treatment groups (P < 0.05 APAP vs. sham or APAP + 3-AB), indicating substantial liver tissue damage. There was no statistically significant difference in the ALT and AST values in the APAP + 3-AB group compared to the sham group (Table 1).

3.3. Serum neopterin levels

The APAP group exhibited significantly increased serum NP levels (P < 0.05, APAP vs. the other groups). The APAP + 3-AB group had significantly decreased serum NP levels in comparison to the APAP group, but serum neopterin remained elevated in the APAP + 3-AB relative to the sham group (P < 0.05, APAP + 3-AB group vs. other groups) (Table 1).

3.4. Serum NOx levels

Serum NOx levels in the APAP group were increased significantly relative to the other experimental groups (P < 0.05, APAP vs. sham or APAP + 3-AB). The APAP + 3-AB treatment group had significantly decreased serum NOx levels relative to the APAP group, but increased levels relative to the sham treatment group (P < 0.05, APAP + 3-AB group vs. APAP and sham group) (Table 2).

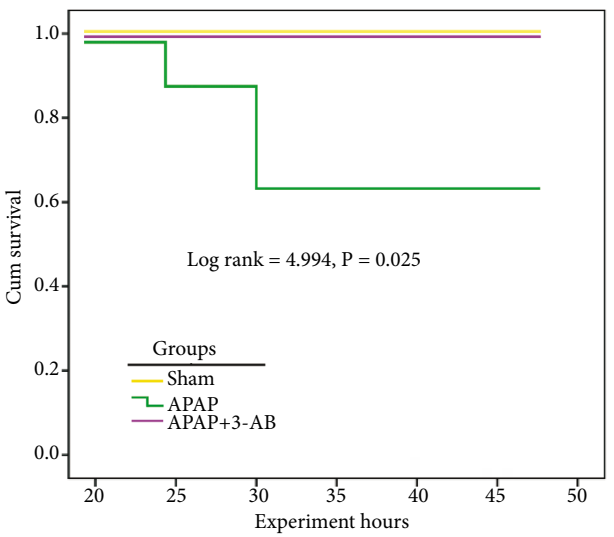

Figure 1. Survival rates in the groups.

Table 1. Biochemical parameters in the groups.

	Sham	APAP	APAP + 3-AB
	(N = 10)	(N = 10)	(N = 10)
ALT (U/L)	74.0 ± 18.6	1263.8 ± 264.6 [a]	126.0 ± 58.8 [a, b]
AST (U/L)	148.0 ± 29.8	586.0 ± 152.6 [a]	236.0 ± 51.4 [a, b]
Neopterin (nM/L)	4.2 ± 1.4	15.2 ± 1.8 [a]	7.2 ± 1.5 [b]

[a]: P < 0.05, statistically different from sham group.
[b]: P < 0.05, statistically different from APAP group.

3.5. Tissue lipid peroxidation levels

MDA levels in the APAP group were significantly increased in comparison to the other treatment groups, indicating increased hepatocellular damage (P < 0.05, APAP vs. sham or APAP + 3-AB). However, MDA levels were significantly decreased in the APAP + 3-AB group compared to the APAP group (P < 0.05, APAP + 3-AB vs. APAP) (Table 2).

3.6. Tissue antioxidant enzyme activities

The total tissue SOD activity in the APAP and APAP + 3-AB groups was significantly increased relative to the sham treatment group (P < 0.05, APAP and APAP + 3-AB vs. sham treatment). The total tissue SOD activity was significantly greater in the APAP + 3-AB group in comparison to the APAP treatment group (P < 0.05, APAP + 3-AB treatment vs. APAP treatment) (Table 2).

GSH-Px activity was significantly decreased in the APAP treatment group in comparison to the sham-operated group (P < 0.05, APAP treatment alone vs. sham group). GSH-Px activity was significantly greater in the APAP + 3-AB treatment group in comparison to the APAP group, but decreased relative to the sham-operated group (P < 0.05, APAP + 3-AB vs. sham and APAP) (Table 2).

3.7. Histopathologic findings

Blinded histological examination did not detect any characteristics of liver or kidney injury in the sham-operated group. Conversely, all of the animals in the APAP treatment group exhibited severe liver injury with marked central necrosis, hemorrhaging, leukocyte infiltration, and all indicators of hepatotoxicity. In the APAP + 3-AB treatment group, hepatic injury parameters, including necrosis and leukocyte infiltration, were significantly less prevalent than in the animals treated with APAP alone (P < 0.05, APAP + 3-AB vs. APAP) (Table 3; Figure 2).

4. Discussion

Hepatotoxicity due to APAP overdose was first reported by Davidson and Eastham (48). They performed a

Table 2. Tissue peroxidation and antioxidant parameters in the groups.

	Sham	APAP	APAP + 3-AB
	(N = 10)	(N = 10)	(N = 10)
MDA (mM/g protein)	0.59 ± 0.13	1.86 ± 0.52 a	0.95 ± 0.12 a, b
SOD (U/g protein)	662.28 ± 212.56	248.44 ± 82.60 a	396.58 ± 82.36 a, b
GSH-Px (U/g protein)	66.28 ± 11.24	20.24 ± 5.36 a	40.34 ± 4.84 a, b
NOx (U/L)	4.10 ± 1.53	8.92 ± 1.76 a	5.26 ± 1.28 a, b

[a]: $P < 0.05$, statistically different from sham group.
[b]: $P < 0.05$, statistically different from APAP group.

Table 3. Pathologic scores. Data are expressed as median (min–max).

Groups	Sham (N = 10)	APAP (N = 10)	APAP + 3-AB (N = 10)
Edema	0 (0–1)	3 (2–4) [a]	2 (1–2)[a]
Hemorrhage	0 (0–1)	3 (2–-6) [a]	2 (1–-4)[a, b]
Leukocyte infiltration	0 (0–1)	3 (2–5) [a]	1 (1–2)[a, b]
Ballooning (prenecrotic change)	0 (0–0)	6 (2–7) [a]	2 (1–3)[a, b]
Total score	0 (0–3)	15 (8–22) [a]	7 (4–11) [a, b]

[a]: $P < 0.05$, statistically different from sham group.
[b]: $P < 0.05$, statistically different from APAP group.

histological examination of a large number of liver sections demonstrating fulminant hepatic necrosis. This necrosis was located primarily in the centrilobular tissues. This landmark publication described for the first time eosinophilic degeneration of hepatocytes with pyknosis of the nuclear material, and vacuolization and early degenerative changes in the peripheral cells surrounding the portal areas. The cases described exhibited mild polymorphonuclear leukocytic infiltration with fulminant necrosis confined primarily to the hepatocytes of the centrilobular regions of the liver

Prescott et al. published a thorough report of the clinical and biochemical characteristics in clinical cases of APAP toxicity, demonstrating a distinct increase in serum ALT and AST activities, mild hyperbilirubinemia, and a significant increase in prothrombin clotting time (49). Other clinical reports have suggested that a delayed elimination half-life of APAP may contribute to increased hepatotoxicity at high dosages (50). In some cases, nephrotoxicity may develop in addition to hepatotoxicity (51,52).

The overall clinical features of APAP-induced hepatotoxicity and the pathogenesis of associated congestion and coagulative necrosis have been well characterized. However, the mechanistic understanding of this disease is less well developed. Laskin (53,54) proposed that the interaction between parenchymal and nonparenchymal cells is a critical event in the development of APAP-induced centrilobular necrosis. Nonparenchymal cells, such as Kupffer cells, are a significant source of chemotactic factors and generate a substantial quantity of reactive oxygen intermediates that are responsible for the hepatic acute phase response (55,56). However, histopathological examination is a more effective measure of changes in vascular congestion and hepatocellular necrosis (57).

To the best of our knowledge, the current study is among the first to demonstrate the therapeutic benefits of 3-AB in treating APAP-induced hepatotoxicity. In addition, this study incorporates unique parameters in APAP-induced toxicity, such as survival rate and serum neopterin. Our results demonstrate that the inhibition of PARP with 3-AB had a significant protective effect against APAP-induced pathology and related serum markers. 3-AB treatment was also associated with a reduction in hepatic oxidative stress in accordance with the histopathological findings.

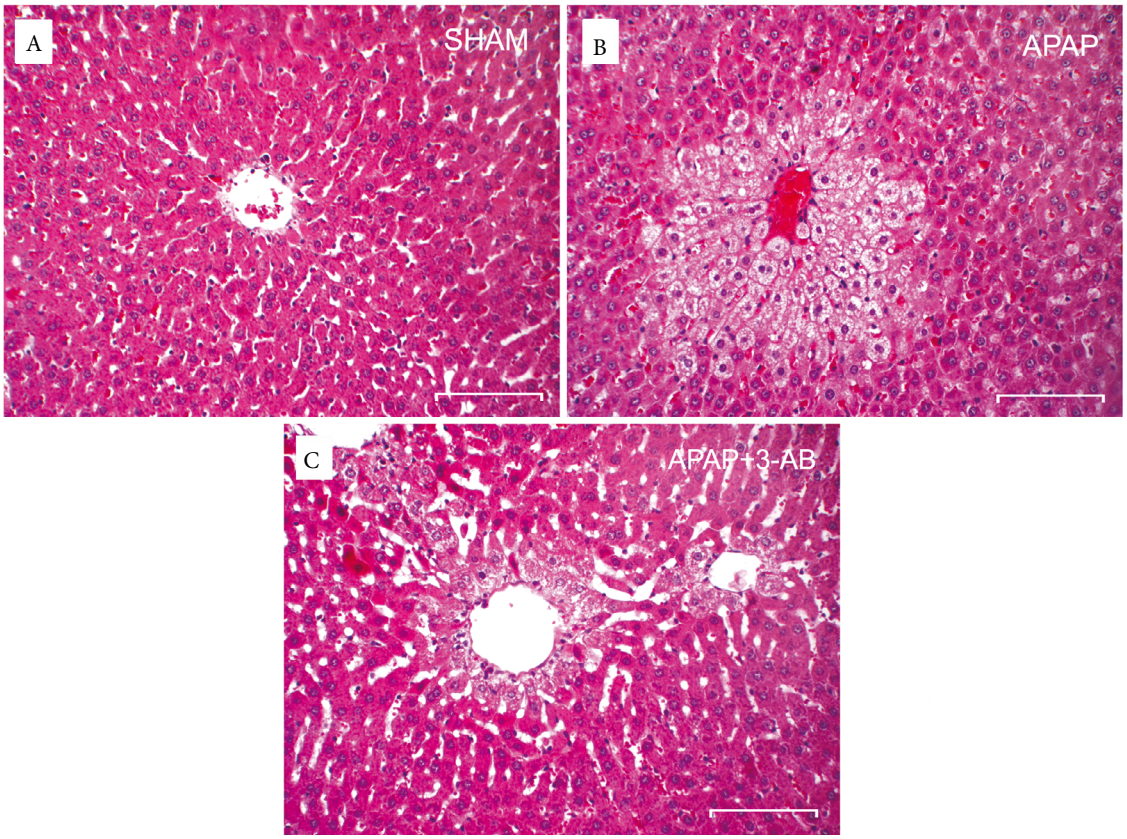

Figure 2. A) Representative photograph from sham group showing normal hepatocytes and a central vein. B) Photograph from APAP group, with massive edema and ballooning (prenecrotic degeneration) of pericentral hepatocytes. C) Photograph from APAP + 3-AB group, where inhibition of PARP with 3-AB treatment normalized edema and ballooning. H&E, scale bars = 200 µm.

Modulation of serum NP and decreased serum AST and ALT were observed in the animals treated with 3-AB following APAP-induced hepatotoxicity, but not in the animals treated with APAP alone. Most importantly, 3-AB treatment significantly increased APAP-induced hepatic injury survival. Together, these findings demonstrate that 3-AB administration is protective against the significant effects of APAP-induced hepatotoxicity.

The reduction in tissue MDA (an oxidative stress marker) levels and GSH-Px activity levels, and the increase in SOD enzymatic activity, suggest that the inhibition of PARP by 3-AB limited necrotic damage and the depletion of metabolic cofactors such as NAD, preventing oxidative injury.

The administration of 3-AB ameliorated APAP-induced inflammation and injury in both hepatic and renal tissues. We propose that PARP inhibition enables improved maintenance of intracellular energy stores. When hepatic cells are exposed to toxic levels of APAP, the formation of NAPQI is known to result in DNA fragmentation and other macromolecular distortion within the cytoplasm. This DNA fragmentation represents a significant mutagenic event and requires the use of cellular energy stores to prevent subsequent cell necrosis. This necrotic process may be prevented with a PARP inhibitor such as 3-AB; however, in the later stages PARP inhibition may have to be terminated to allow for the continuation of DNA repair processes.

Elevated ALT and AST activities are well-known indicators of liver damage. (58). Necrotic damage to the liver causes leakage of AST and ALT through the hepatocellular membrane and into the bloodstream. Although elevated concentrations of liver enzymes in the serum may indicate hepatocellular damage, AST and ALT are poor prognostic indicators of the severity of liver injury (59). Others have reported the elevation of serum NP levels in the rat model of APAP-induced liver injury in a dose-dependent manner (60). In the present study, we demonstrate that the elevation of liver enzymes and NP levels associated with APAP-induced hepatotoxicity is inhibited by the PARP inhibition activities of 3-AB, in correlation with the histopathological findings. NP

is a critical indicator of cellular immunity produced by monocytes/macrophages in response to the cytokine interferon-γ. NP expression is associated with varying stages of disease progression (61). Our observation of decreased NP levels in the APAP + 3-AB treatment group suggests that administration of 3-AB may impair the recruitment of monocytes and macrophages to the liver tissue. The histological observation of decreased leucocyte infiltration among the APAP + 3-AB treatment group compared to the animals receiving APAP alone supports this hypothesis.

PARP inhibition with 3-AB was associated with significant improvements in liver function, as evidenced by reduction in serum GGT, ALT, and AST levels among animals treated with APAP. Decreased severity of hepatic injury likely resulted in reduced leakage of liver enzymes into the serum.

Peroxynitrite formation occurs in APAP-induced liver injury and may contribute to later pathological hepatocellular events (19). Peroxynitrite is a strong oxidant that is highly reactive with most biological molecules (31). In the current study, serum NOx levels were elevated among the animals receiving APAP alone compared to the sham treatment group. However, therapeutic treatment with 3-AB resulted in decreased serum and tissue NOx relative to animals treated with APAP alone. PARP inhibition thus had a beneficial effect in directly or indirectly decreasing excessive NOx production in injured hepatocytes. The prevention of inflammatory and necrotic processes through PARP inhibition may impair the generation of superoxide radicals that react with NO to yield the highly hepatotoxic molecule peroxynitrite.

Protein expression will enhance the understanding of the molecular processes involved in the alleviation of APAP-induced hepatotoxicity by PARP inhibition. The effects of 3-AB on mitochondrial function may be critical in elucidating the therapeutic effects of PARP inhibition at the molecular level. Additional benefits of 3-AB treatment in injured liver tissue may be attributable to the modulation of inflammatory pathways and the altered expression of cytokines and antioxidant enzymes.

In conclusion, this study demonstrates that 3-AB protects against APAP-induced hepatic injury in rats.

References

1. Yaman H, Isbilir S, Cakir E, Uysal B. Current issues with paracetamol induced toxicity. J Exp Integr Med 2011; 1: 165–166.
2. Murali A, Ashok P, Madhavan H. Hepatoprotective effect of *Hemidesmus indicus* var. *pubescens* leaf extract on paracetamol induced hepatic damage. Medicinal Chemistry & Drug Discovery 2012; 3: 103–115.
3. Lee WM. Acetaminophen and the U.S. Acute Liver Failure Study Group: lowering the risks of hepatic failure. Hepatology 2004; 40: 6–9.
4. Jollow DJ, Mitchell JR, Potter WZ, Davis DC, Gillette JR, Brodie BB. Acetaminophen-induced hepatic necrosis. Role of covalent binding in vivo. J. Pharmacol Exp Therap 1973; 187: 195–202.
5. Mitchell JR, Jollow DJ, Potter WZ, Davis DC, Gillette JR, Brodie BB. Acetaminophen-induced hepatic necrosis. Role of drug metabolism. J Pharmacol Exp Ther 1973; 187: 185–194.
6. Potter WZ, Davis DC, Mitchell JR, Jollow DJ, Gillette JR, Brodie BB. Acetaminophen-induced hepatic necrosis. Cytochrome p-450-mediated covalent binding in vitro. J Pharmacol Exp Ther 1973; 187: 203–210.
7. Farber JL, Leonard TB, Kyle ME, Nakae D, Serroni A, Rogers SA. Peroxidation-dependent and peroxidation-independent mechanisms by which acetaminophen kills cultured rat hepatocytes. Arch Biochem Biophys 1980; 267: 640–650.
8. Gerson RJ, Casini A, Gilfor D, Serroni A, Farber JL. Oxygen-mediated cell injury in the killing of cultured hepatocytes by acetaminophen. Biochem Biophys Res Commun 1980; 126: 1129–1137.
9. Pacifici GM, Back DJ. Sulphation and glucuronidation of paracetamol in human liver: assay conditions. Biochem Pharmacol 1988; 37: 4405–4407.
10. Nelson SD. Mechanisms of the formation and disposition of reactive metabolites that can cause acute liver injury. Drug Metab Rev 1995; 27: 147–177.
11. Anbarasu C, Rajkapoor B, Kalpana J. Protective effect of *Pisonia aculeata* on paracetamol induced hepatotoxicity in rats. J Exp Integr Med 2011; 1: 167–172.
12. Nelson SD. Molecular mechanisms of the hepatotoxicity caused by acetaminophen. Semin Liver Dis 1990; 10: 267–278.
13. Cohen SD, Khairallah EA. Selective protein arylation and acetaminophen-induced hepatotoxicity. Drug Metab Rev 1997; 29: 59–77.
14. Qiu Y, Benet LZ, Burlingame AL. Identification of hepatic protein targets of the reactive metabolites of the non-hepatotoxic regioisomer of acetaminophen, 3′-hydroxyacetanilide, in the mouse in vivo using two-dimensional gel electrophoresis and mass spectrometry. Adv Exp Med Biol 2001; 500: 663–673.
15. Tirmenstein, MA, Nelson SD. Subcellular binding and effects on calcium homeostasis produced by acetaminophen and a nonhepatotoxic regioisomer, 3′-hydroxyacetanilide, in mouse liver. J Biol Chem 1989; 264: 9814–9819.
16. Meyers LL, Beierschmitt WP, Khairallah EA, Cohen SD. Acetaminophen-induced inhibition of mitochondrial respiration in mice. Toxicol Appl Pharmacol 1988; 93: 378–387.
17. Ramsay RR, Rashed MS, Nelson SD. In vitro effects of acetaminophen metabolites and analogs on the respiration of mouse liver mitochondria. Arch Biochem Biophys 1989; 273: 449–457.

18. Jaeschke H. Glutathione disulfide formation and oxidant stress during acetaminophen-induced hepatotoxicity in mice in vivo: The protective effect of allopurinol. J Pharmacol Exp Ther 1990; 255: 935–941.

19. Knight TR, Kurtz A, Bajt ML, Hinson JA, Jaeschke H. Vascular and hepatocellular peroxynitrite formation during acetaminophen-induced liver injury: role of mitochondrial oxidant stress. Toxicol Sci 2001; 62: 212–220.

20. Knight TR, Ho YS, Farhood A, Jaeschke H. Peroxynitrite is a critical mediator of acetaminophen hepatotoxicity in murine livers: protection by glutathione. J Pharmacol Exp Ther 2002; 303: 468–475.

21. Adams ML, Pierce RH, Vail ME, White CC, Tonge RP, Kavanagh TJ, Fausto N, Nelson SD, Bruschi SA. Enhanced acetaminophen hepatotoxicity in transgenic mice overexpressing BCL-2. Mol Pharmacol 2001; 60: 907–915.

22. Knight TR, Jaeschke H. Acetaminophen-induced inhibition of Fas receptor-mediated liver cell apoptosis: Mitochondrial dysfunction versus glutathione depletion. Toxicol Appl Pharmacol 2002; 181: 133–141.

23. Kon K, Kim JS, Jaeschke H, Lemasters JJ. Mitochondrial permeability transition in acetaminophen-induced necrotic and apoptotic cell death to cultured mouse hepatocytes. Hepatology 2004; 40: 1170–1179.

24. Ray SD, Sorge CL, Raucy JL, Corcoran GB. Early loss of large genomic DNA in vivo with accumulation of Ca^{2+} in the nucleus during acetaminophen-induced liver injury. Toxicol Appl Pharmacol 1990; 106: 346–351.

25. Ray SD, Kamendulis LM, Gurule MW, Yorkin RD, Corcoran GB. Ca^{2+} antagonists inhibit DNA fragmentation and toxic cell death induced by acetaminophen. FASEB J 1993; 7: 453–463.

26. Shen W, Kamendulis LM, Ray SD, Corcoran GB. Acetaminophen-induced cytotoxicity in cultured mouse hepatocytes: effects of Ca^{2+}-endonuclease, DNA repair, and glutathione depletion inhibitors on DNA fragmentation and cell death. Toxicol Appl Pharmacol 1992; 112: 32–40.

27. Gujral JS, Knight TR, Farhood A, Bajt ML, Jaeschke H. Mode of cell death after acetaminophen overdose in mice: apoptosis or oncotic necrosis? Toxicol Sci 2002; 67: 322–328.

28. Lawson JA, Fisher MA, Simmons CA, Farhood A, Jaeschke H. Inhibition of Fas receptor (CD95)-induced hepatic caspase activation and apoptosis by acetaminophen in mice. Toxicol Appl Pharmacol 1999; 156: 179–186.

29. Jahr S, Hentze H, Englisch S, Hardt D, Fackelmayer FO, Hesch RD, Knippers R. DNA fragments in the blood plasma of cancer patients: quantitations and evidence for their origin from apoptotic and necrotic cells. Cancer Res 2001; 61: 1659–1665.

30. Liaudet L. Poly(adenosine 5'-diphosphate) ribose polymerase activation as a cause of metabolic dysfunction in critical illness. Curr Opin Clin Nutr Metab Care 2002; 5: 175–184.

31. Pacher P, Beckman JS, Liaudet L. Nitric oxide and peroxynitrite in health and disease. Physiol Rev 2007; 87: 315–424.

32. Erdelyi K, Bakondi E, Gergely P, Szabo C. Pathophysiologic role of oxidative stress-induced poly(ADP-ribose) polymerase-1 activation: focus on cell death and transcriptional regulation. Cell Mol Life Sci 2005; 62: 751–759.

33. Cover C, Fickert P, Knight TR, Fuchsbichler A, Farhood A, Trauner M, Jaeschke H. Pathophysiological role of poly(ADP-ribose) polymerase (PARP) activation during acetaminophen-induced liver cell necrosis in mice. Toxicol Sci 2005; 84: 201–208.

34. Kroger H, Ehrlich W, Klewer M, Gratz R, Dietrich A, Miesel R. The influence of antagonists of poly(ADP-ribose) metabolism on acetaminophen hepatotoxicity. Gen Pharmacol 1996; 27: 167–170.

35. Oztas E, Guven A, Türk E, Uysal B, Akgül EO, Cayci T, Ersoz N, Korkmaz A. 3-Aminobenzamide, a poly ADP ribose polymerase inhibitor, attenuates renal ischemia/reperfusion injury. Ren Fail 2009; 31: 393–399.

36. Yasar M, Uysal B, Kaldirim U, Oztas Y, Sadir S, Ozler M, Topal T, Coskun O, Kilic A, Cayci T et al. Poly(ADP-ribose) polymerase inhibition modulates experimental acute necrotizing pancreatitis-induced oxidative stress, bacterial translocation and neopterin concentrations in rats. Exp Biol Med 2010; 235: 1126–1133.

37. Graziani G, Szabó C. Clinical perspectives of PARP inhibitors. Pharmacol Res 2005; 52: 109–118.

38. Purnell MR, Whish WJ. Novel inhibitors of poly(ADP-ribose) synthetase. Biochem J 1980; 185: 775–777.

39. Karlberg T, Hammarström M, Schütz P, Scensson L, Schüler H. Crystal structure of the catalytic domain of human PARP2 in complex with PARP inhibitor ABT-888. Biochemistry 2010; 49: 1056–1058.

40. Chattopadhyay RR, Sarkar SK, Ganguly S, Banerjee RN, Basu TK, Mukherjee A. Hepatoprotective activity of *Azadirachta indica* leaves on paracetamol induced hepatic damage in rats. Indian J Exp Biol 1992; 30: 738–740.

41. Lowry OH, Rosebrough NJ, Farr AL, Randall RJP. Protein measurement with the Folin phenol reagent. J Biol Chem 1951; 193: 265–275.

42. Ohkawa H, Ohishi H, Yagi K. Assay for lipid peroxides in animal tissues by thiobarbituric reaction. Anal Biochem 1979; 95: 351–358.

43. Durak I, Yurtarslani Z, Canbolat O, Akyol O. A methodological approach to superoxide dismutase (SOD) activity assay based on inhibition of nitroblue tetrazolium (NBT) reduction. Clin Chim Acta 1993; 214: 103–104.

44. Paglia DE, Valentine WN. Studies on the quantitative and qualitative characterization of erythrocyte glutathione peroxidase. J Lab Clin Med 1967; 70: 158–169.

45. Alrashed M, Abougoush M, Akgul EO, Erbil MK. Detection method of serum and urine neopterin levels by high performance liquid chromatography and clinical applications. Gulhane Medical Journal 2002; 44: 273–277.

46. Koca K, Yurttas Y, Bilgic S, Cayci T, Topal T, Durusu M, Kaldirim U, Akgul EO, Ozkan H, Yanmis I et al. Effect of preconditioned hyperbaric oxygen and ozone on ischemia-reperfusion induced tourniquet in skeletal bone of rats. J Surg Res 2010; 164: 83–89.

47. Gul H, Uysal B, Cakir E, Yaman H, Macit E, Yildirim AO, Eyi YE, Kaldirim U, Oztas E, Akgul EO et al. The protective effects of ozone therapy in a rat model of acetaminophen-induced liver injury. Environ Toxicol Pharmacol 2012; 34: 81–86.

48. Davidson DG, Eastham WN. Acute liver necrosis following overdose of paracetamol. Br Med J 1966; 5512: 497–499.

49. Dixon MF, Nimmo J, Prescott LF. Experimental paracetamol-induced hepatic necrosis: a histopathological study. J Pathol 1971; 103: 225–229.

50. Schiodt FV, Ott P, Christensen E, Bondesen S. The value of plasma acetaminophen half-life in antidote-treated acetaminophen overdosage. Clin Pharmacol Ther 2002; 71: 221–225.

51. Boyer TD, Rouff SL. Acetaminophen-induced hepatic necrosis and renal failure. JAMA 1971; 218: 440–441.

52. Prescott LF, Roscoe P, Wright N, Brown SS. Plasma-paracetamol half-life and hepatic necrosis in patients with paracetamol overdosage. Lancet 1971; 1: 519–522.

53. Laskin DL. Parenchymal and nonparenchymal cell interactions in hepatotoxicity. Adv Exp Med Biol 1990; 283: 499–505.

54. Laskin DL. Role of macrophages and endothelial cells in hepatotoxicity. In: Billiar TR, Curran RD, editors. Hepatocyte and Kupffer Cell Interactions. Boca Raton, FL, USA: CRC Press; 1992. pp. 147–168.

55. Billiar TR, Curran RD, Williams DL, Kispert PH. Liver nonparenchymal cells are stimulated to provide interleukin 6 for induction of the hepatic acute-phase response in endotoxemia but not in remote localized inflammation. Arch Surg 1992; 127: 31–37.

56. Ramadori G, Van Damme J, Rieder H, Meyer zum Buschenfelde KH. Interleukin 6, the third mediator of acute-phase reaction, modulates hepatic protein synthesis in human and mouse. Comparison with interleukin 1 beta and tumor necrosis factor-alpha. Eur J Immunol 1988; 18: 1259–1264.

57. Blazka ME, Wilmer JL, Holladay SD, Wilson RE, Luster MI. Histopathology of acetaminophen-induced liver changes: role of interleukin 1 alpha and tumor necrosis factor alpha. Toxicol Pathol 1996; 24: 181–189.

58. Bruss M, Homann J, Molderings GJ. Dysferlinopathy as an extrahepatic cause for the elevation of serum transaminases. Medizinische Klinik 2004; 99: 326–329 (article in German with English abstract).

59. Huang L, Heinloth AN, Zeng ZB, Paules RS, Bushel PR. Genes related to apoptosis predict necrosis of the liver as a phenotype observed in rats exposed to a compendium of hepatotoxicants. BMC Genomics 2008; 9: 288.

60. Demirbas S, Cakir E, Akgul EO, Seyrek M, Cayci T, Kurt YG, Uysal B, Aydin I, Kurt B, Yaman H et al. Elevated serum neopterin levels in acetaminophen-induced liver injury. Environ Toxicol Pharmacol 2011; 31: 165–170.

61. Kaufmann P, Tilz GP, Demel U, Wachter H, Kreijs GJ, Fuchs D. Neopterin plasma concentrations predict the course of severe acute pancreatitis. Clin Chem Lab Med 1998; 36: 29–34.